Manuscript - Published at *The IES Journal Part A: Civil & Structural Engineering, Vol. 4, No. 3, August 2011, 143-156.*

Responses of interconnected floating bodies

L. Sun[a], R. Eatock Taylor[*a,b] and Y. S. Choo[a]

[a] *Centre for Offshore Research & Engineering and Department of Civil Engineering, National University of Singapore, Singapore 117576*
[b] *Department of Engineering Science, University of Oxford, Oxford OX1 3PJ, UK*

(Received 18 August 2010; final version received XX Month Year)

This paper describes an investigation of the wave induced responses of constrained multiple bodies. The hydrodynamic analysis is based on linear diffraction theory, and the constraints in the connections between the bodies are imposed by the Lagrange multiplier technique. Results are given for two cases of two rectangular boxes connected by a hinge and by a rigid rod, which are compared with published data. An example of a tanker alongside an FLNG barge is then considered, and the effect of the constraints on the responses is assessed.

Keywords: constrained bodies; hydrodynamic interactions; closely spaced vessels

1. Introduction

Offshore operations are frequently based on use of two or more vessels in close proximity, and increasingly it is required to join these vessels with structural connections. At one extreme these might be the fenders with spring and breast lines connecting a floating liquid natural gas (LNG) tanker to a floating LNG (FLNG) processing barge; at the other, the connection might be a stiff truss joining two barges in a catamaran configuration (as discussed by Cheung, 2010). Examples relating to installation are the twin barge float-over configurations described by Tahar et al. (2004) in relation to the Benguela Belize feasibility study; and by Edelson et al. (2008) for the Kikeh spar deck installation. The use of such configurations for platform removal is also now an active area of interest.

A crucial capability in the design of such systems, alongside physical experiments, is the ability to model numerically multiple floating bodies linked by rigid or flexible constraints. The hydrodynamic modelling involves multi-body

* Corresponding author. Email: r.eatocktaylor@eng.ox.ac.uk

diffraction analysis; and the response analysis requires suitable representation of the constrained multi-body dynamics. There are two distinct methods of tackling this. One is to solve the hydrodynamics problem first, for the bodies allowed to respond freely in all of their rigid body degrees of freedom (i.e. six times the number of bodies). Wave forcing as well as added mass and damping coefficients are evaluated, involving hydrodynamic coupling between the bodies. Dynamic coupling (by rigid or flexible structures, including possible hinges and universal joints etc) is then incorporated in the formulation of the equations of motion. A systematic treatise on the formulation of constrained dynamic systems (without the fluid) is that by Shabana (2010). In the marine context, examples of the application of this effectively two-stage approach have been given by Langley (1984), Kral and Kreuzer (1999) and O´'Catha´in et al. (2008). The second method of analysis solves the coupled problem directly, using the mode expansion technique (Newman 1994, Lee and Newman 2000, Taghipour and Moan 2008). For large systems involving many bodies, such as the wave energy converter investigated by Taghipour and Moan, the second method would appear to be the more efficient (as fewer radiation problems need to be solved within the hydrodynamic analysis). For systems with complex constraints, however, the first method offers greater flexibility. We have therefore based the analysis here on that two-stage formulation.

The hydrodynamics of closely spaced multiple bodies in waves is itself a non-trivial problem to analyse, and some very complex behaviour can arise. For two long vessels in a side-by-side arrangement, near-standing waves can be excited along the narrow gap between the vessels. The phenomenon can be triggered by incident waves at discrete frequencies and from any direction, even beam seas. It has recently been systematically studied by Sun et al (2010a) for the case of two side-by-side

rectangular box-shaped barges. Earlier investigations include the work of Hong et al. (2005), Koo and Kim (2005), Kashiwagi (2007) and Pauw et al. (2007). Sun et al. (2010b) have also studied the problem for an LNG tanker alongside a large FLNG barge. Here we use the same configuration (originating in the EU Safe Offload Project) to investigate the effect of differing degrees of constraint between the vessels.

The paper is arranged as follows. The next section describes how the constraints are built in to the analysis, using the Lagrange multiplier technique. In view of the requirement to be able to model elastic interconnections, the problem is formulated *ab initio* as one of an elastic system (which is assumed here to be linear). The resulting equations are linked to the diffraction analysis code DIFFRACT (Eatock Taylor and Chau 1992, Zang et al. 2006, Sun et al. 2010b). Section 3 applies the methodology to the interconnected body configuration considered by Newman (1994) using the mode expansion technique, thereby providing validation of the present formulation. This is followed by the analysis of the FLNG-tanker arrangement, and some conclusions.

2. Formulation of the constrained equations

We are concerned here with the linear response of N interconnected rigid bodies when excited by unidirectional regular waves at frequency ω. The rigid body equations of motion are first considered in the absence of any rigid constraints. The $6N$ exciting forces and corresponding displacements may be written

$$\mathbf{F}(t) = \mathrm{Re}[\mathbf{f}(\omega)]\exp(\mathrm{i}\omega t); \Xi(t) = \mathrm{Re}[\boldsymbol{\xi}(\omega)]\exp(\mathrm{i}\omega t)\,. \tag{1}$$

After removing the harmonic time factor we may then express the equations of motion in the form

$$\left\{-\omega^2[\mathbf{A}+\mathbf{A}_H(\omega)]+\mathrm{i}\omega[\mathbf{B}+\mathbf{B}_H(\omega)]+[\mathbf{C}+\mathbf{C}_H]\right\}\boldsymbol{\xi}=\mathbf{f}\,. \tag{2}$$

Here the matrix **A** is the rigid body mass matrix for the N bodies. Damping and stiffness matrices **B** and **C** respectively correspond to any connections coupling the degrees of freedom. Matrix $\mathbf{C}_H$ represents the hydrostatic restoring coefficients. Matrices $\mathbf{A}_H$ and $\mathbf{B}_H$ involve hydrodynamic coefficients which are the added mass and damping matrices obtained by solving $6N$ radiation problems. Here these, and the wave exciting forces and moments **f**, are evaluated by the computer program DIFFRACT. This is based on quadratic boundary element panelling of the submerged surfaces of the bodies. Sun et al. (2010b) provide details, and examples of validation, including discussion of the suppression of irregular frequencies and the application of the code to multiple bodies responding independently.

For convenience we write Equation (2) in the simplified form

$$\mathbf{K}\boldsymbol{\xi}=\mathbf{f}, \tag{3}$$

where of course the matrix **K** and also the vectors $\boldsymbol{\xi}$ and **f** depend on frequency. Under the assumptions made, this is the Euler equation corresponding to taking the variation of a functional

$$\Pi=\tfrac{1}{2}\boldsymbol{\xi}^T\mathbf{K}\boldsymbol{\xi}-\boldsymbol{\xi}^T\mathbf{f} \tag{4}$$

where superscript T denotes the transpose.

We now assume that there are rigid constraints between some of the degrees of freedom, given by the constraint equation

$$\mathbf{D}\xi = 0. \tag{5}$$

This may be imposed in the variational formulation by augmenting the function Π by means of Lagrangian multipliers λ, leading to the modified functional

$$\Pi = \tfrac{1}{2}\xi^T\mathbf{K}\xi - \xi^T\mathbf{f} + \lambda^T\mathbf{D}\xi\,. \tag{6}$$

If there are n degrees of freedom in the unconstrained case and m constraints, then the size of the vectors and matrices are as follows: $\mathbf{f}$ and ξ are (n×1); $\mathbf{K}$ is (n×n); $\mathbf{D}$ is (m×n); and λ is (m×1). Taking the variations with respect to ξ and λ leads to

$$\begin{pmatrix} \mathbf{K} & \mathbf{D}^T \\ \mathbf{D} & \mathbf{0} \end{pmatrix}\begin{pmatrix} \xi \\ \lambda \end{pmatrix} = \begin{pmatrix} \mathbf{f} \\ \mathbf{0} \end{pmatrix}. \tag{7}$$

Equation (7) may be solved directly for the displacements ξ and Lagrangian multipliers λ, which are generalized forces corresponding to the constraints.

This may be illustrated for a simple problem. Consider two interconnected floating barges, constrained to have the same sway ($\xi_2 = \xi_8$, say, but with no other degrees of freedom affected). The constraint matrix is then

$$\mathbf{D} = \begin{bmatrix} 0 & 1 & 0 & 0 & 0 & 0 & 0 & -1 & 0 & 0 & 0 & 0 \end{bmatrix}_{1\times 12} \tag{8}$$

i.e. n=12, m=1, and λ is the force in the connection.

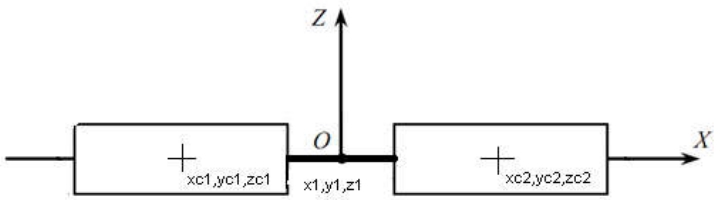

Figure 1. Two floating barges with rigid connection

A more realistic case, illustrated schematically in Figure 1, is that of two floating barges constrained by a rigid connection, so that they both have the same response at some arbitrary point on the connection. There are thus 6 constraints (m=6), and the constraint matrix (transpose) is

$$\mathbf{D}_{12\times 6}^{T} = \begin{pmatrix} 1 & 0 & 0 & 0 & 0 & 0 \\ 0 & 1 & 0 & 0 & 0 & 0 \\ 0 & 0 & 1 & 0 & 0 & 0 \\ 0 & -(z_1 - z_{c1}) & y_1 - y_{c1} & 1 & 0 & 0 \\ z_1 - z_{c1} & 0 & -(x_1 - x_{c1}) & 0 & 1 & 0 \\ -(y_1 - y_{c1}) & x_1 - x_{c1} & 0 & 0 & 0 & 1 \\ -1 & 0 & 0 & 0 & 0 & 0 \\ 0 & -1 & 0 & 0 & 0 & 0 \\ 0 & 0 & -1 & 0 & 0 & 0 \\ 0 & z_1 - z_{c2} & -(y_1 - y_{c2}) & -1 & 0 & 0 \\ -(z_1 - z_{c2}) & 0 & x_1 - x_{c2} & 0 & -1 & 0 \\ y_1 - y_{c2} & -(x_1 - x_{c2}) & 0 & 0 & 0 & -1 \end{pmatrix} \tag{9}$$

Here (x_{c1}, y_{c1}, z_{c1}) and (x_{c2}, y_{c2}, z_{c2}) are the global coordinates of the centres of rotation of each body, and (x_1, y_1, z_1) is the point at which they are connected.

These two examples illustrate the simplicity of this approach for applying rigid constraints between multiple bodies. It should also be recalled that flexible constraints may also be incorporated, by means of the stiffness matrix **C** in Equation (2).

3. Responses of interconnected barges

We now examine a problem that has been previously solved by Newman (1994) using the mode expansion technique. It concerns two rectangular barges, each of length (L) 40 m, beam (B) 10 m and draft 5 m and having uniform mass distribution. They are connected end-to-end by a bar of length 10 m, having a hinge half way along which allows rotation about a horizontal axis parallel to the ends of the barges. The water depth is assumed to be infinite.

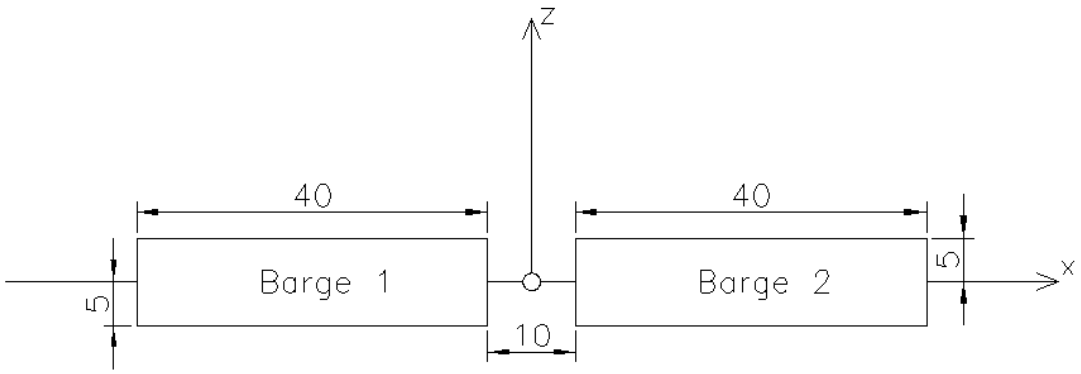

Figure 2. Geometry of two barges connected by hinged bar (Newman 1994)

The geometry is shown in Figure 2 (with lengths in meters). In this case the constraint matrix (transpose) is

$$\mathbf{D}_{12\times 5}^{T} = \begin{pmatrix} 1 & 0 & 0 & 0 & 0 \\ 0 & 1 & 0 & 0 & 0 \\ 0 & 0 & 1 & 0 & 0 \\ 0 & 0 & 0 & 1 & 0 \\ 0 & 0 & -25 & 0 & 0 \\ 0 & 25 & 0 & 0 & 1 \\ -1 & 0 & 0 & 0 & 0 \\ 0 & -1 & 0 & 0 & 0 \\ 0 & 0 & -1 & 0 & 0 \\ 0 & 0 & 0 & -1 & 0 \\ 0 & 0 & -25 & 0 & 0 \\ 0 & 25 & 0 & 0 & -1 \end{pmatrix} . \qquad (10)$$

The boundary element meshes used for the hydrodynamic analysis are shown in Figure 3. One plane of symmetry is exploited in the analysis. The meshes on the inner free surfaces are required because of the special form of integral equation used in the boundary element analysis DIFFRACT: this avoids the need to compute the solid angle at each nodal point, and also provides the means for suppressing the well known effects of irregular frequencies (the details of the implementation of this feature in DIFFRACT are given in Sun et al 2010b, based on Sun et al 2008).

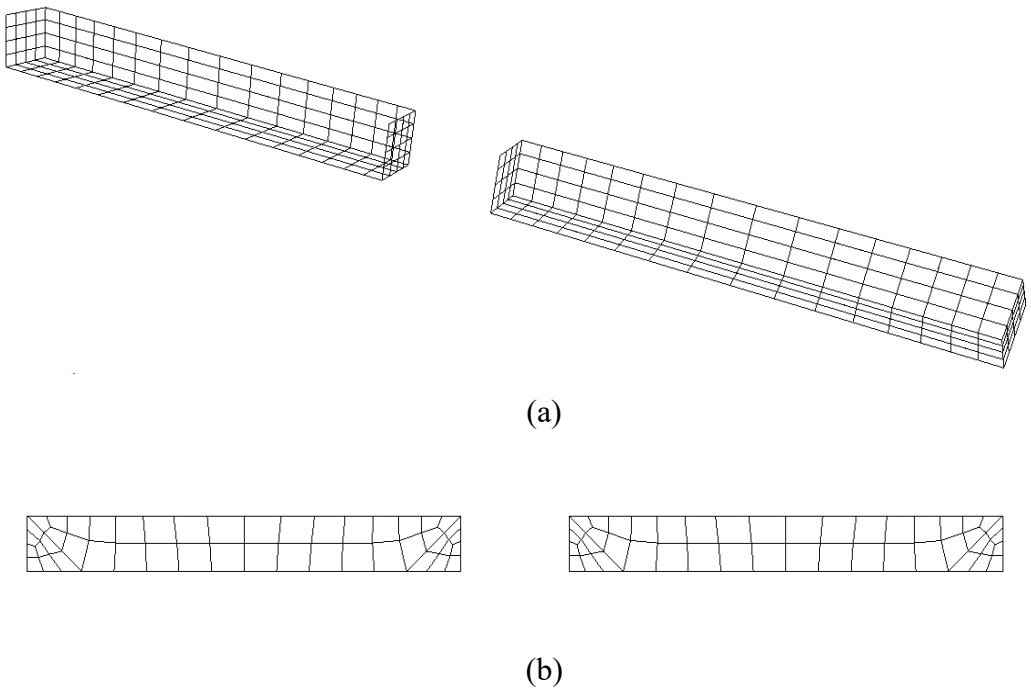

Figure 3. Boundary element meshes for two floating rectangular boxes:
(a) mesh on the submerged body surfaces; (b) mesh on the inner free surfaces.

Figure 4 shows the results for certain frequency responses of the hinged barge motions, for the case of waves in the x-direction in Figure 2 (head seas). These are compared with values digitised from the published plots in Newman (1994), where the results are plotted against wave period. Figure 4a shows the vertical motion of the hinge non-dimensionalised by the wave amplitude A; while Figure 4b shows the hinge rotation, non-dimensionalised by $2KA$ to be consistent with the result plotted by

Newman (1994). Here K is the deep water wave number. The comparisons are generally good, apart from a small oscillation in the curves just below the period T=6 s. This might be linked to the resolution of the plots: here we used a spacing of ΔT=0.1 s. It should be noted that the circles in these figures identifying the results from Newman correspond to the points we have digitised from the published graphs, which show continuous lines.

Results were also obtained for the case where the barges are rigidly joined by the interconnecting bar. This corresponds to Figure 1, and the constraint matrix in Equation (9) after appropriate substitution of the geometric parameters. The corresponding comparison with Newman's results for the vertical motion at the mid-point of the bar is given in Figure 5. Again the agreement appears satisfactory.

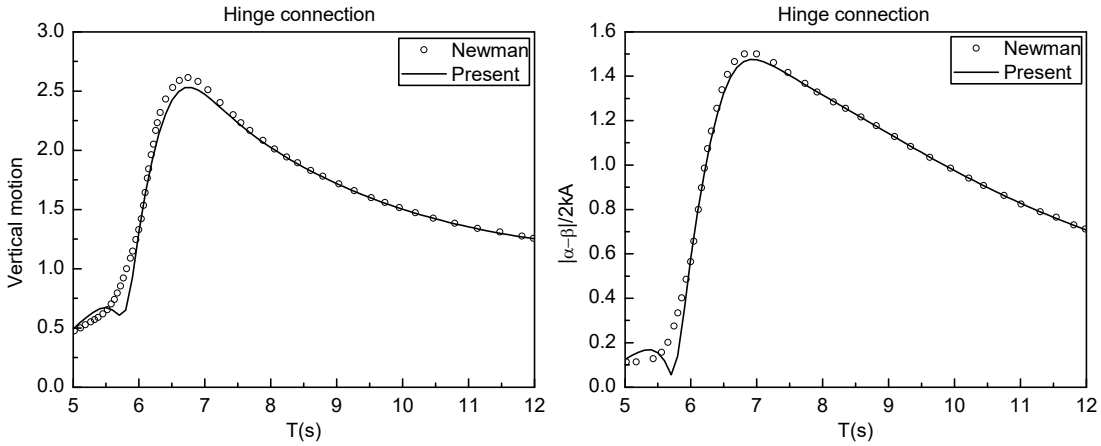

Figure 4. Motions of hinged barges: (a) vertical motion at the hinge; (b) rotation of hinge.

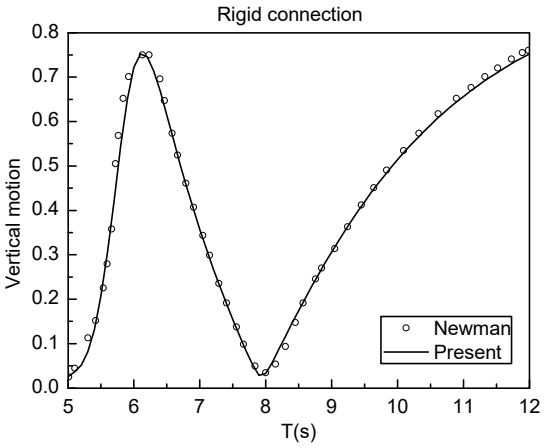

Figure 5. Motions of rigidly connected barges

As mentioned following Equation (7), the solution technique we have adopted yields directly the forces in the constraint, without the need for supplementary calculations based on the motions. It is therefore very easy to obtain, say, the vertical force in the hinge, or in the bar for the rigidly connected barges (i.e. the shear force). In each case this would correspond to the solution for λ_3. Figure 6 shows the results obtained from our analysis of these vertical forces, again plotted against wave period (they have been non-dimensionalised by $\rho gALB$, where ρ is the fluid density and g is the acceleration due to gravity). It is seen that the vertical force is the same, regardless of the presence or absence of the hinge. This may at first sight seem surprising: after all, the vertical responses are very different in these two cases. The behaviour can, however, be easily explained as follows. The vertical forces in the connection between the vessels are due to three effects: the wave exciting forces; the inertia forces due to the vessel responses; and the hydrodynamic radiation forces (added mass and damping effects) also due to the vessel responses. The wave forces are the same, with or without the hinge. The other forces can be separated into components linked to modes of response that are symmetric about the vertical plane through the hinge; and those linked to anti-symmetric modes. Because of the geometric symmetry

in the problem, the responses in the symmetric and anti-symmetric modes are uncoupled. The introduction of the hinge on the plane of symmetry only affects the symmetric modes of response. Only the anti-symmetric modes, however, contribute to the vertical force. Therefore this force is unaffected by the presence of the hinge.

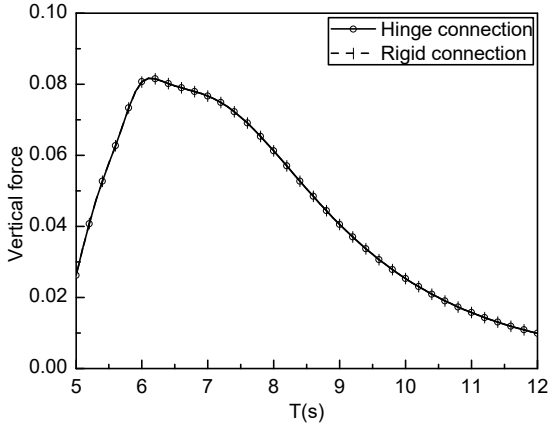

Figure 6. Vertical force in the bar connecting the two barges, for hinged and rigid cases

4. Results for FLNG-tanker configuration

Sun et al. (2010b) have given comprehensive results for a tanker alongside an FLNG barge, one of the case studies in the EU Safe Offload collaborative project involving industry, research institutes and universities. These results included linear and second order predictions of wave exciting forces, motion responses (where relevant) and free surface elevations in the narrow gap between the vessels. Two cases were considered, with the vessels held fixed; and with the vessels free to respond independently in their rigid body degrees of freedom. Here we extend that analysis to cases where there is an idealised connection between the vessels (but not a complete mooring system with fenders, spring lines and breast lines). The aim is to investigate three simplified generic cases, in beam seas: in the first two cases, the connections are equivalent to those considered above, hinged and rigid. In the third additional case, we have

assumed that the two vessels are permitted to respond in all their degrees of freedom, but there is a horizontal spring connecting them, coupling their sway and roll motions. This is a simple representation of the fenders separating the vessels.

The complete specification of the geometric and dynamic properties of the vessels is given in Sun et al. (2010b). The FLNG barge is a rectangular box of length 400m, breadth 70 m and draught 21.254 m. The tanker is of length 276 m, maximum beam 25.5 m, and draught 11.4 m. They are parallel to each other, with a gap of just 4 m separating them (the dimensions of the design fender). As each vessel has fore-aft symmetry, the geometry involved in the analysis can be simplified to that depicted in Figure 7. Figures 7a and 7b indicate the two beam sea arrangements, with the tanker up-wave (Beam Sea-1) or down-wave (Beam Sea-2) of the FLNG barge. The associated boundary element meshes are shown in Figure 8. The hydrodynamic analysis is of course based on the assumptions of potential flow. In order however to calculate realistic values of roll (and coupled sway), we have incorporated additional roll damping coefficients representing viscous effects, using values provided by Noble Denton (2007).

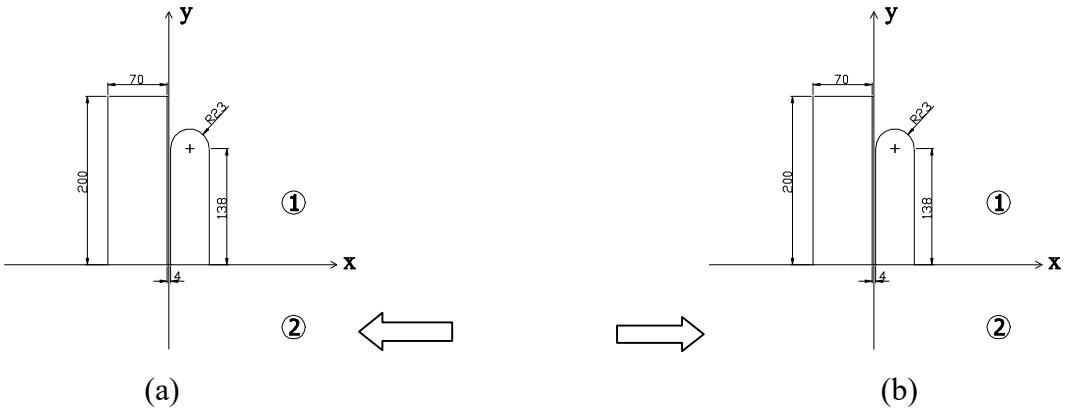

Figure 7. Configuration of FLNG and tanker: (a) Beam Sea-1; (b) Beam Sea-2

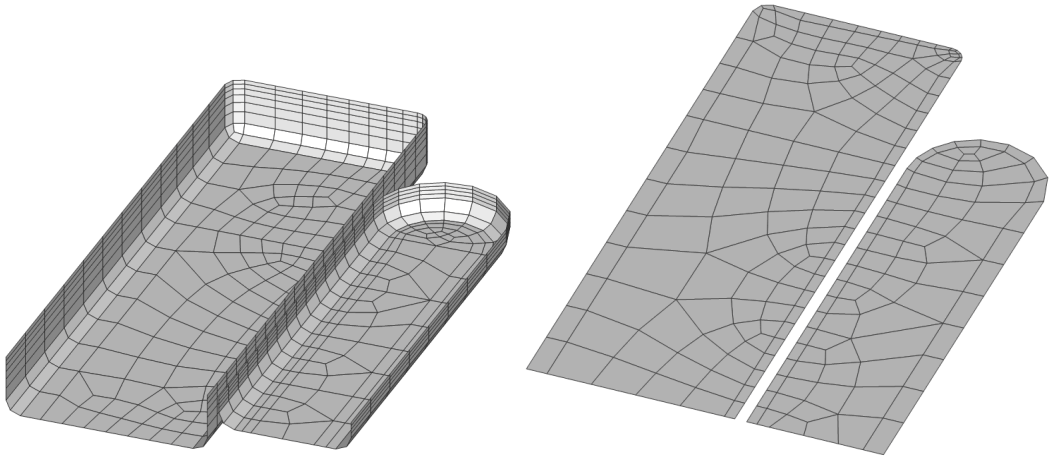

(a) (b)

Figure 8 Meshes on the (a) body surfaces and (b) the inner free surfaces

We consider 4 cases numbered as follows:

1. both vessels free to respond independently
2. vessels attached by a hinge connection
3. vessels attached by a rigid connection
4. vessels attached by a horizontal spring connection.

The stiffness matrix **C** corresponding to the additional spring connection (see Equation (2)) depends on the spring stiffness k, and the vertical distance between the horizontal spring and the centroids of the two vessels, z_f and z_t for the FLNG and tanker respectively. The matrix is then:

$$\mathbf{C} = \begin{bmatrix} k & 0 & 0 & 0 & kz_f & 0 & -k & 0 & 0 & 0 & -kz_t & 0 \\ 0 & 0 & 0 & 0 & 0 & 0 & 0 & 0 & 0 & 0 & 0 & 0 \\ 0 & 0 & 0 & 0 & 0 & 0 & 0 & 0 & 0 & 0 & 0 & 0 \\ 0 & 0 & 0 & 0 & 0 & 0 & 0 & 0 & 0 & 0 & 0 & 0 \\ kz_f & 0 & 0 & 0 & kz_f^2 & 0 & -kz_f & 0 & 0 & 0 & -kz_f z_t & 0 \\ 0 & 0 & 0 & 0 & 0 & 0 & 0 & 0 & 0 & 0 & 0 & 0 \\ -k & 0 & 0 & 0 & -kz_f & 0 & k & 0 & 0 & 0 & kz_t & 0 \\ 0 & 0 & 0 & 0 & 0 & 0 & 0 & 0 & 0 & 0 & 0 & 0 \\ 0 & 0 & 0 & 0 & 0 & 0 & 0 & 0 & 0 & 0 & 0 & 0 \\ 0 & 0 & 0 & 0 & 0 & 0 & 0 & 0 & 0 & 0 & 0 & 0 \\ -kz_t & 0 & 0 & 0 & -kz_f z_t & 0 & kz_t & 0 & 0 & 0 & kz_t^2 & 0 \\ 0 & 0 & 0 & 0 & 0 & 0 & 0 & 0 & 0 & 0 & 0 & 0 \end{bmatrix}$$

corresponding to the 12 degrees of freedom of the FLNG vessel and the tanker respectively. For the majority of the results given here, the value of k is taken as 12.6 MN m^{-1}. This is roughly the linearised stiffness corresponding to four 4.5 m fenders deformed to 60% of their diameter, as deployed in the gap between the vessels in the Safe Offload case study (Noble Denton, 2008). The values of z_f and z_t were 3.854 m and 0.4 m respectively. A few results are also provided to show the effects of different stiffnesses.

Figures 9 – 13 give the results for the configuration Beam Sea-1. In each figure the quantities are plotted against frequency in rad s^{-1}, and correspond to frequency response functions for incident regular waves of unit amplitude. These and the subsequent plots for Beam Sea-2 are characterised by several large peaks at various frequencies. These would be appear to be associated with resonances in the dynamics of the vessels, and resonances due to near-standing wave effects in the narrow gap between the vessels ("near-trapping"). This phenomenon has been extensively investigated by Sun et al. (2010a) for the case of two closely spaced rectangular boxes, with comparisons between numerical results and some simple

analysis. That paper highlights that the most important behaviour in the practically significant lower frequency range is that of standing waves along the gap (even in the case of beam seas). Several standing wave modes can be excited over a narrow range of wave frequencies, with half wavelengths given approximately by the gap length divided by the lowest odd integers. Sun et al (2010b) have shown that similar behaviour is excited in the case of the FLNG and tanker configuration studied here, though of course there is no clear definition of gap length in this case. It is therefore useful to cross-reference the behaviour found in the present paper with the results for wave elevation in the gap given by Sun et al. (2010b).

Figures 9, 10 and 11 give the results for sway, heave and roll motions, with the upper and lower plots showing the results for the FLNG vessel and the tanker respectively. Note that the scales of the results for the tanker and the FLNG vessel in these figures are different. The various lines in these plots relate to the four cases identified above. In Figure 9 there is a sharp peak in the sway of both vessels near ω=0.98 rad s^{-1}, for the freely floating and spring connected arrangements (cases 1 and 4). This frequency lies between two peaks in the gap elevation frequency response for this case, at 0.94 and 1.04 rad s^{-1} respectively. There is no evidence of this peak in sway response for rigid and hinged connections, though there are smaller peaks in the tanker horizontal response just above 0.8 rad s^{-1}. Throughout most of the frequency range plotted there are roughly two patterns of response: cases 1 and 4, and cases 2 and 3 respectively. The major exception to this concerns the large peak in case 4 at 0.21 rad s^{-1}. It seems likely that this is associated with the natural frequency of the mode in which the two vessels connected by the spring move horizontally out of phase. Overall the FLNG sway response is much less affected at the frequencies of the peaks, as might be anticipated because of its much larger inertia.

The heave response of the freely floating tanker, shown in Figure 10b, has a broad peak around 0.52 rad s^{-1}, which is associated with the heave resonance. The corresponding resonance for the FLNG vessel is near 0.47 rad s^{-1}. Similar peaks, but at slightly different frequencies, occur in the other cases. For both the tanker and the FLNG vessel, the effect of the horizontal constraints appears to be to lower slightly the heave resonance frequencies of each vessel; but the rigid connection does not quite make these frequencies equal. As in the case of sway, the heave responses in cases 1 and 4 are rather similar, though the peak at 0.21 rad s^{-1} is rather insignificant in Figure 10b. The other very notable features in Figure 10 are the peaks in the tanker response at just over 0.8 rad s^{-1}. For the case of the rigid connection this is at 0.81 rad s^{-1}, which is the frequency of the largest peak in the frequency response of the free surface elevation in the gap between the freely floating vessels (Figure 21 of Sun et al 2010b). Insertion of the hinge appears to increase the frequency of this peak slightly, and to increase its magnitude substantially. The effects of the free surface motions on the FLNG heave response, however, are again rather small (as for sway).

The roll motions are presented in Figure 11. These also show large resonant motions, which in this mode are expected in practice to be significantly influenced by the effects of viscous damping. The relative magnitudes of the peaks shown here are, nevertheless, indicative of the implications of the different coupling arrangements. One can confirm that in the case of the rigid connection the two vessels have the same roll motion, and the frequency of the maximum roll in this case is close to the peak of the heave responses of the FLNG and tanker.

The horizontal force in the connection between the vessels is shown in Figure 12. Results over the full frequency range 0 to 1.6 rad s^{-1} are given in the left hand plot, while the right hand plot shows these in greater detail between 0.7 and 1.0 rad s^{-1}. This force is also seen to be dominated by peaks at just above 0.8 rad s^{-1}, as was found for the vertical motions. Again case 2 with the hinge gives rise to a substantially higher magnitude of the peak, at a slightly higher frequency. For case 4 with the spring a resonant peak (albeit small) may be seen at 0.21 rad s^{-1}.

Figure 13 shows the vertical force in the hinged and rigid connections, displayed similarly to the results in Figure 12. As in the case of heave motions of each vessel, there are now broad-banded peaks near 0.5 rad s^{-1}, close to the heave resonance frequencies of each vessel. There are also sharp peaks, as in both the vertical motions and in the horizontal connection forces, near 0.8 rad s^{-1}. Now, however, the peak force in the hinged connection is substantially smaller that that in the rigid connection. In the context of this figure, it is worth recalling some discussion in the previous section: if the system has geometric symmetry about the vertical plane containing the hinge, the vertical force is unaffected by the insertion of a hinge in a rigid horizontal connection. Clearly this is not the case here.

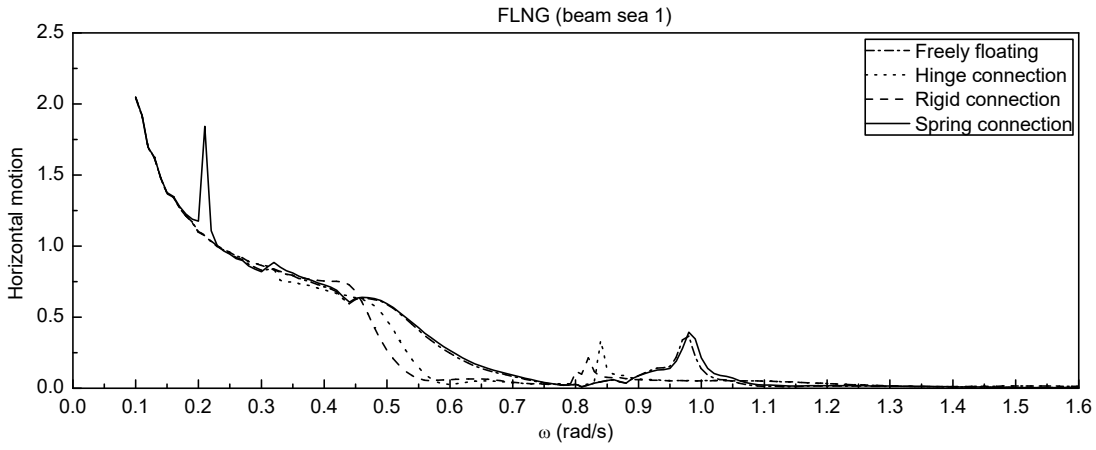

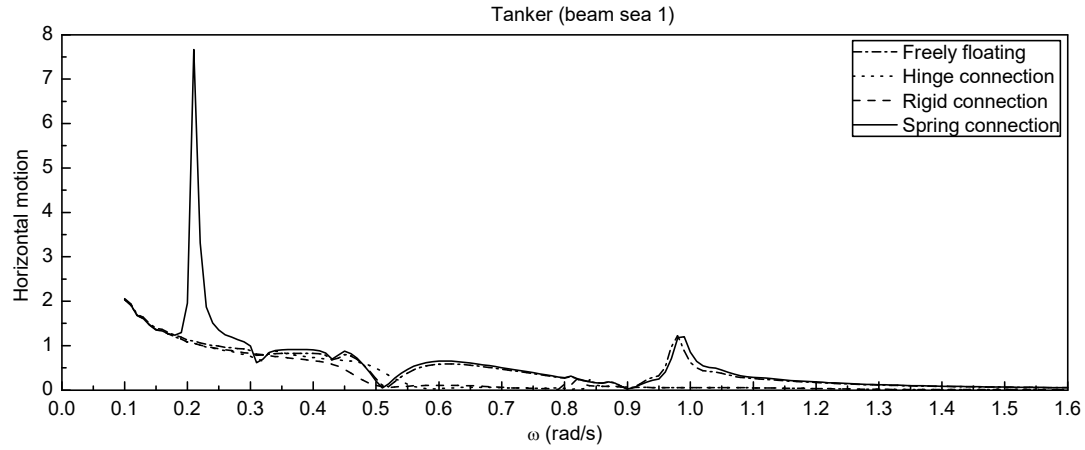

Figure 9. Horizontal responses in Beam Sea-1

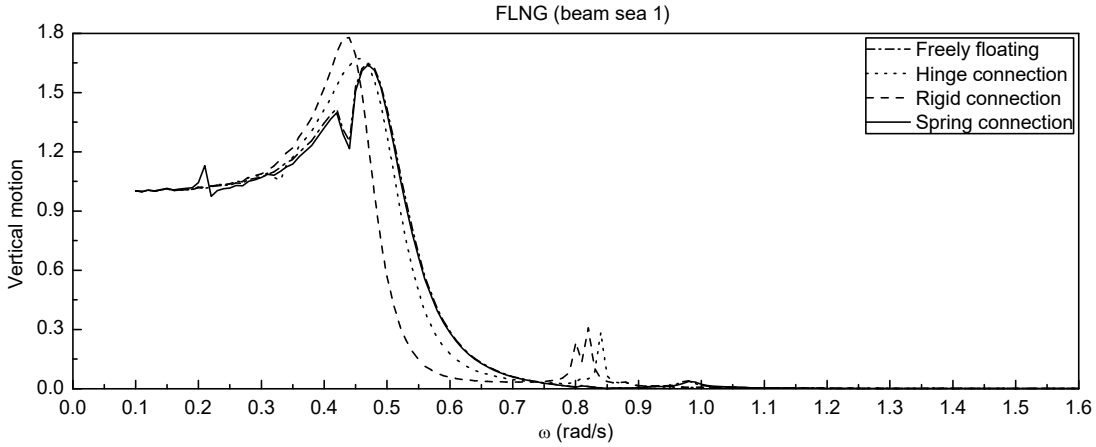

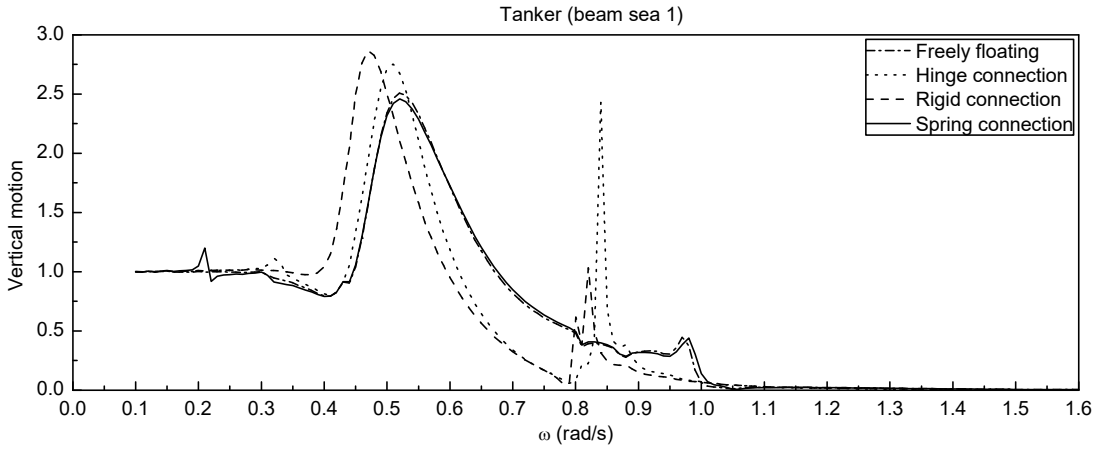

Figure 10. Vertical responses in Beam Sea-1

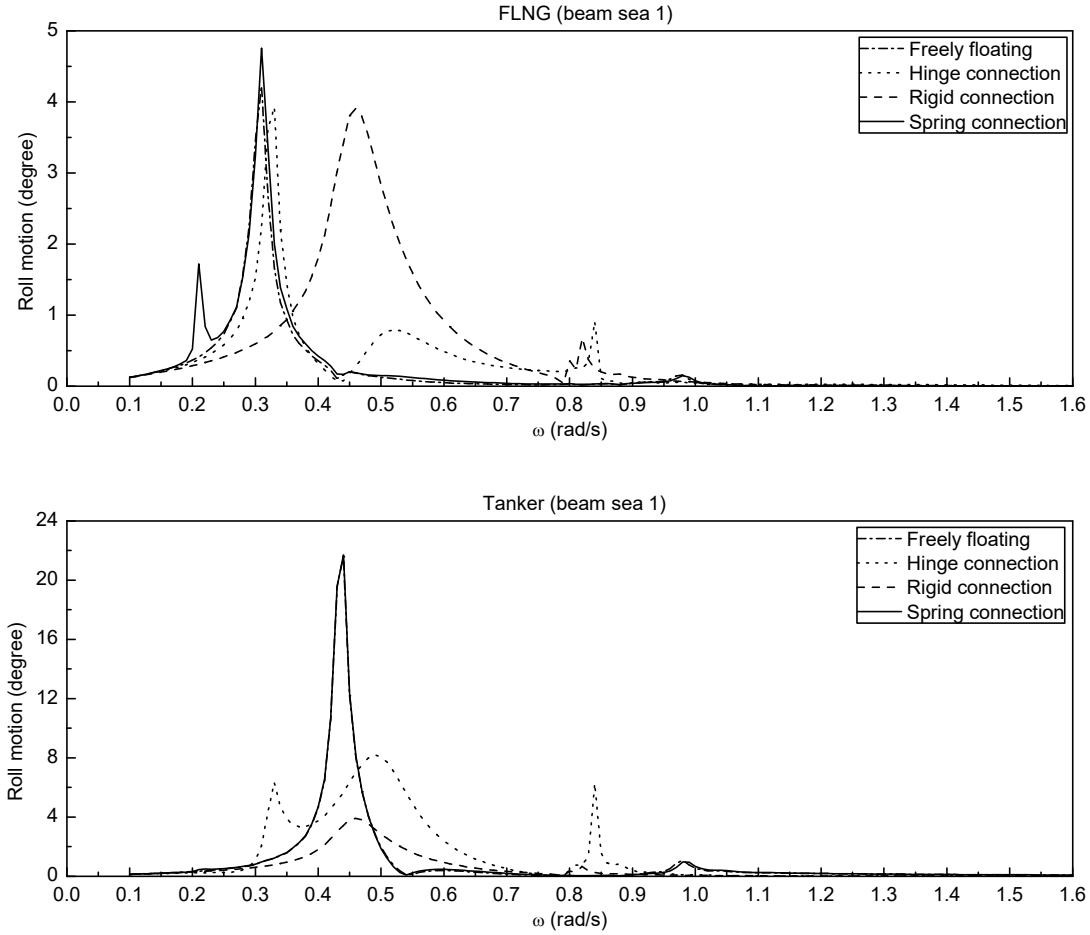

Figure 11. Roll responses in Beam Sea-1

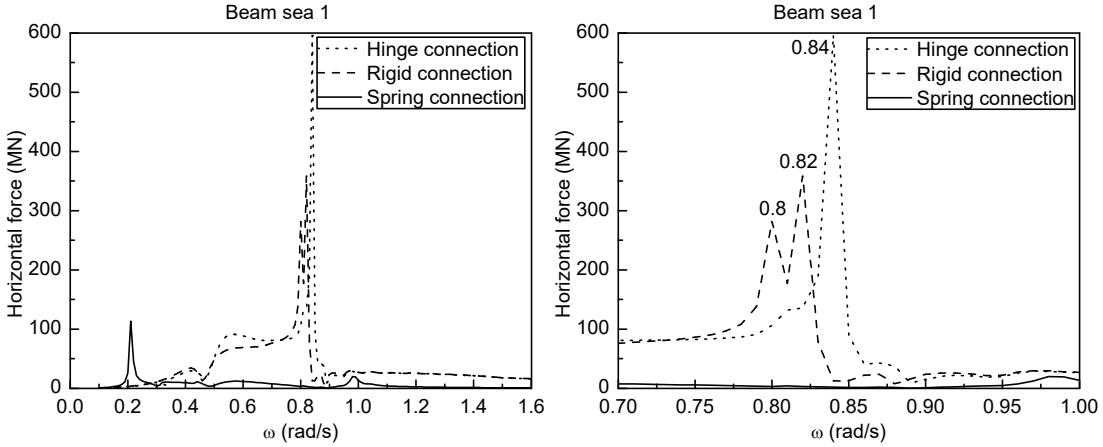

Figure 12. Horizontal force in connection in Beam Sea-1

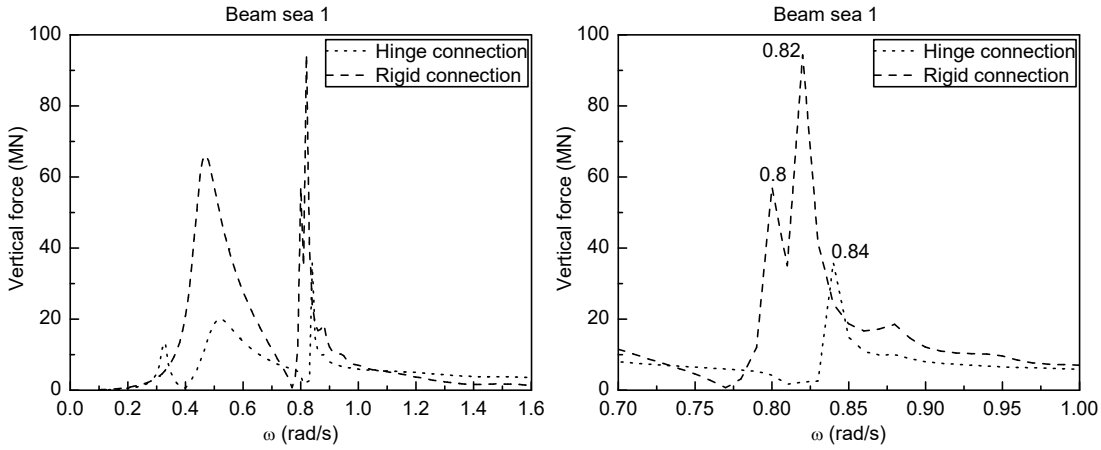

Figure 13. Vertical force in connection in Beam Sea-1

Corresponding results for Beam Sea-2 are shown in Figures 14-18. In this configuration the tanker is on the exposed side of the FLNG. It is found that the pattern of responses is not dissimilar to those discussed above for Beam Sea-1, though the very high peak responses observed in that case are of course substantially reduced by the effect of sheltering in most cases. An exception to this, however, is the large horizontal response seen in Figure 14 for case 4 at 0.21 rad s^{-1}, the resonance associated with the horizontal spring.

Figure 15 shows the vertical responses in Beam Sea-2, in which one may observe that at the heave resonant frequency of the freely floating tanker near 0.52 rad s^{-1}, there is now no peak but rather a reduction in response, which appears to be linked to a neighbouring cancellation frequency. The largest dimensionless vertical motion is just over 1.2, obtained for the spring-connected tanker at 0.21 rad s^{-1}. When the tanker is in the upwave position, the largest peak vertical response (see Figure 10b) is about 2.8 and arises for case 3 at 0.47 rad s^{-1}. There is still a distinctive vertical response in Figure 15b at 0.84 rad s^{-1} for case 2 with the hinge, but its magnitude is about half that found in Beam Sea-1. Similar comments may be made concerning the roll motions shown in Figure 16.

The horizontal force in the connection is shown in Figure 17. The largest peak, is again for case 2 at 0.84 rad s^{-1}, with a magnitude less than half that for Beam Sea-1. The reduction in the vertical force at this frequency, seen in Figure 18, is even greater. There is also a halving of the vertical force for case 2 near the vertical resonance frequency detected with the vessel in the upwave position, 0.51 rad s^{-1}.

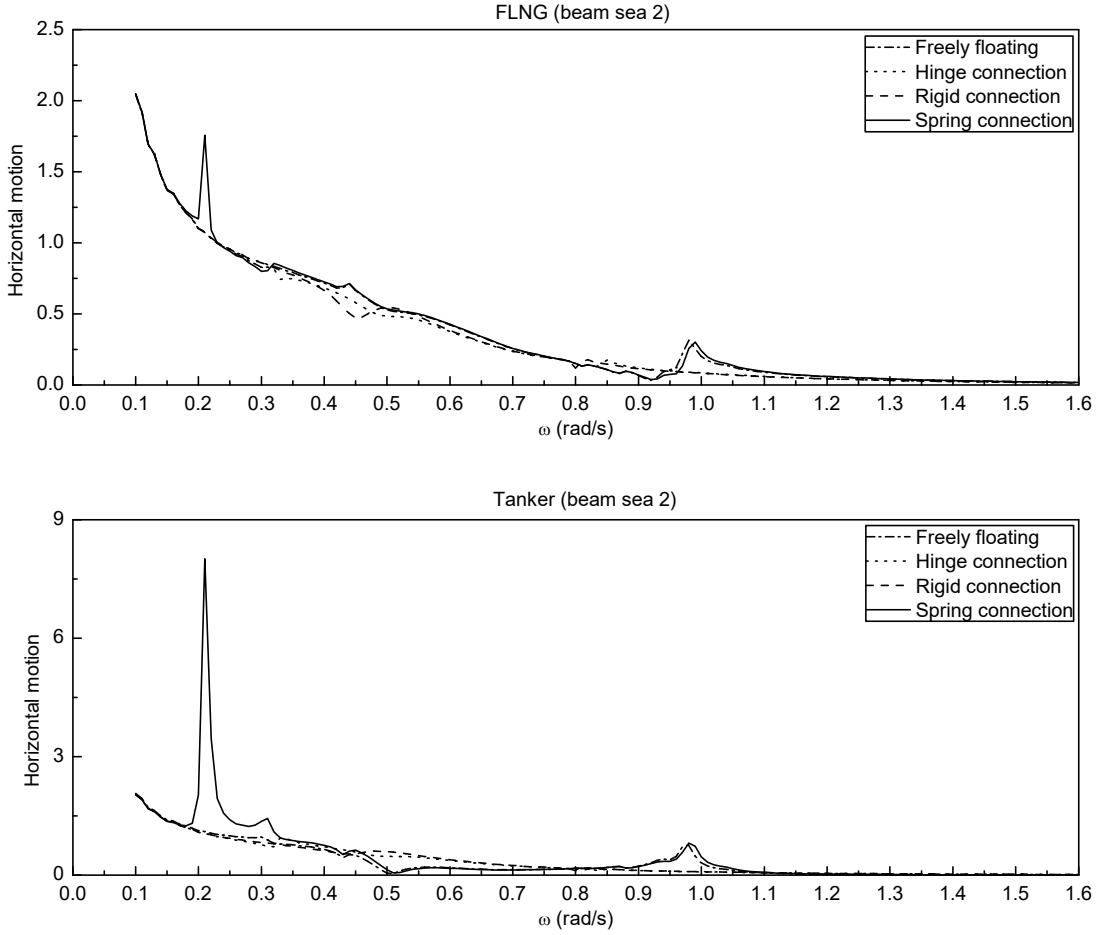

Figure 14. Horizontal responses in Beam Sea-2

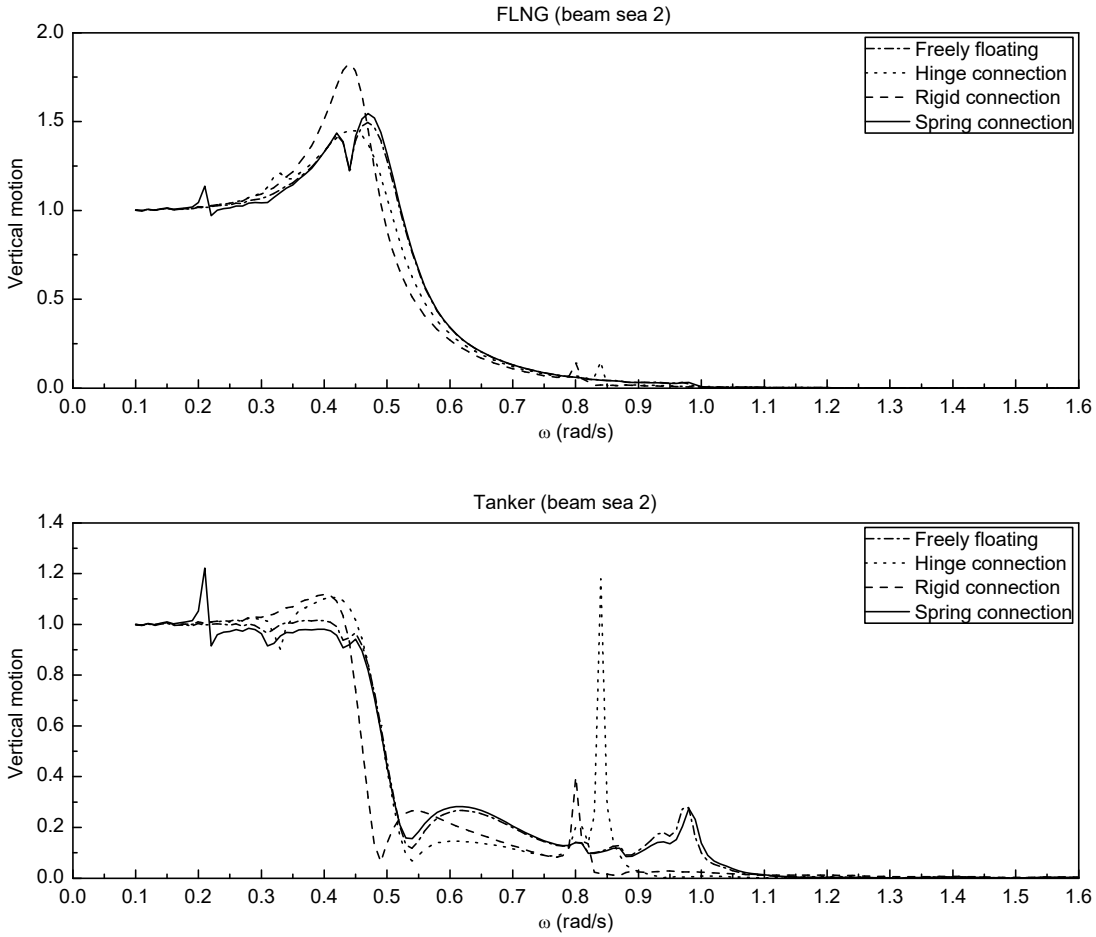

Figure 15. Vertical responses in Beam Sea-2

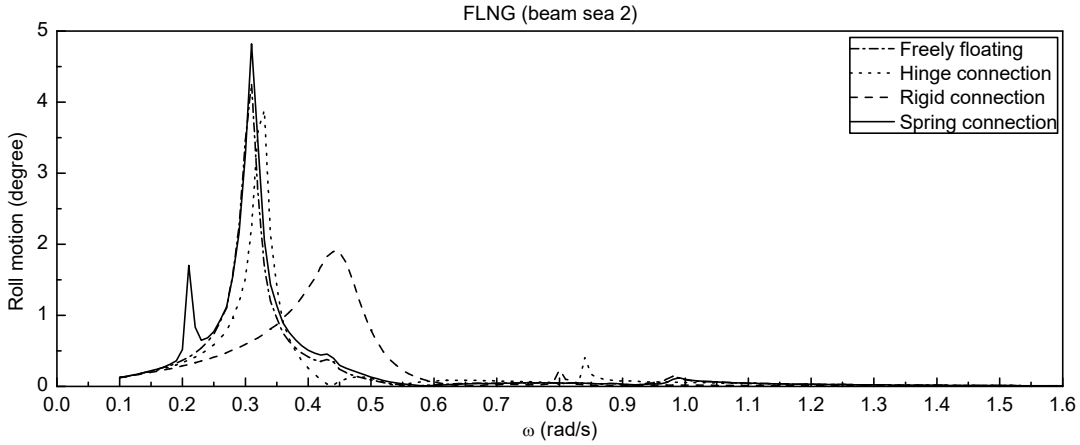

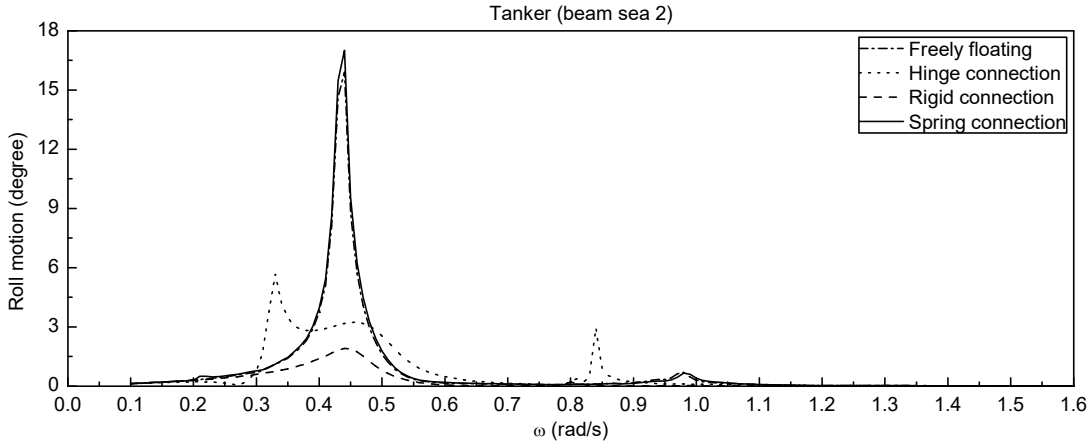

Figure 16. Roll responses in Beam Sea-2

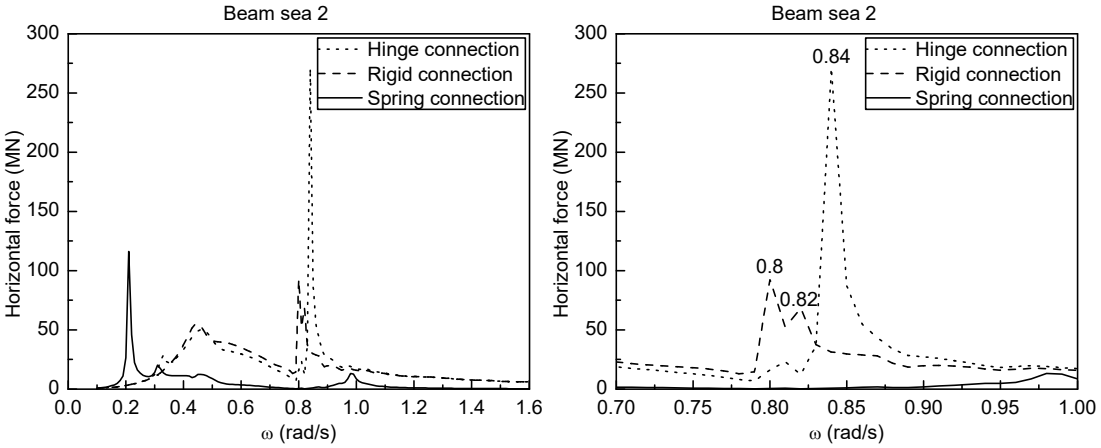

Figure 17. Horizontal force in connection in Beam Sea-2

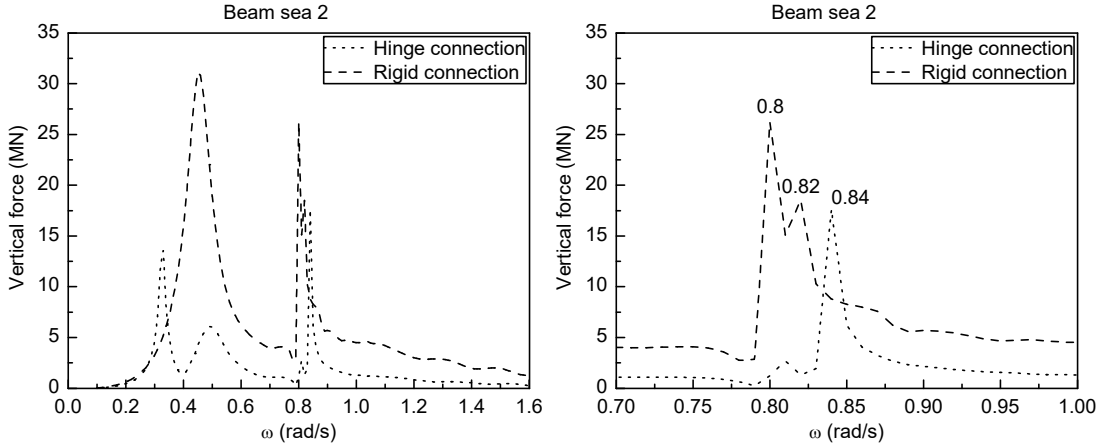

Figure 18. Vertical force in connection in Beam Sea-2

Results showing the influence of different spring stiffnesses on the horizontal motions are shown in Figure 19. This is for Beam Sea-1, the configuration which leads to the greater responses. In addition to the reference case k = 12.6 MNm^{-1} considered in Figure 9, Figure 19 includes results for k = 6.3, 25.2 and 75.0 MNm^{-1}

(the results in Figure 9 for the freely floating case are of course equivalent to $k = 0$, but for clarity these have been omitted from Figure 19). One can confirm that the lowest three resonant peaks below 0.3 rad s^{-1} are at frequencies roughly in the ratio of the square roots of the stiffnesses. The equivalent peak for $k = 75.0$ MNm^{-1} would be just below 0.5 rad s^{-1}, but this can not be seen clearly (perhaps because other effects are now dominating the horizontal motions - note the cancellations in the tanker responses)

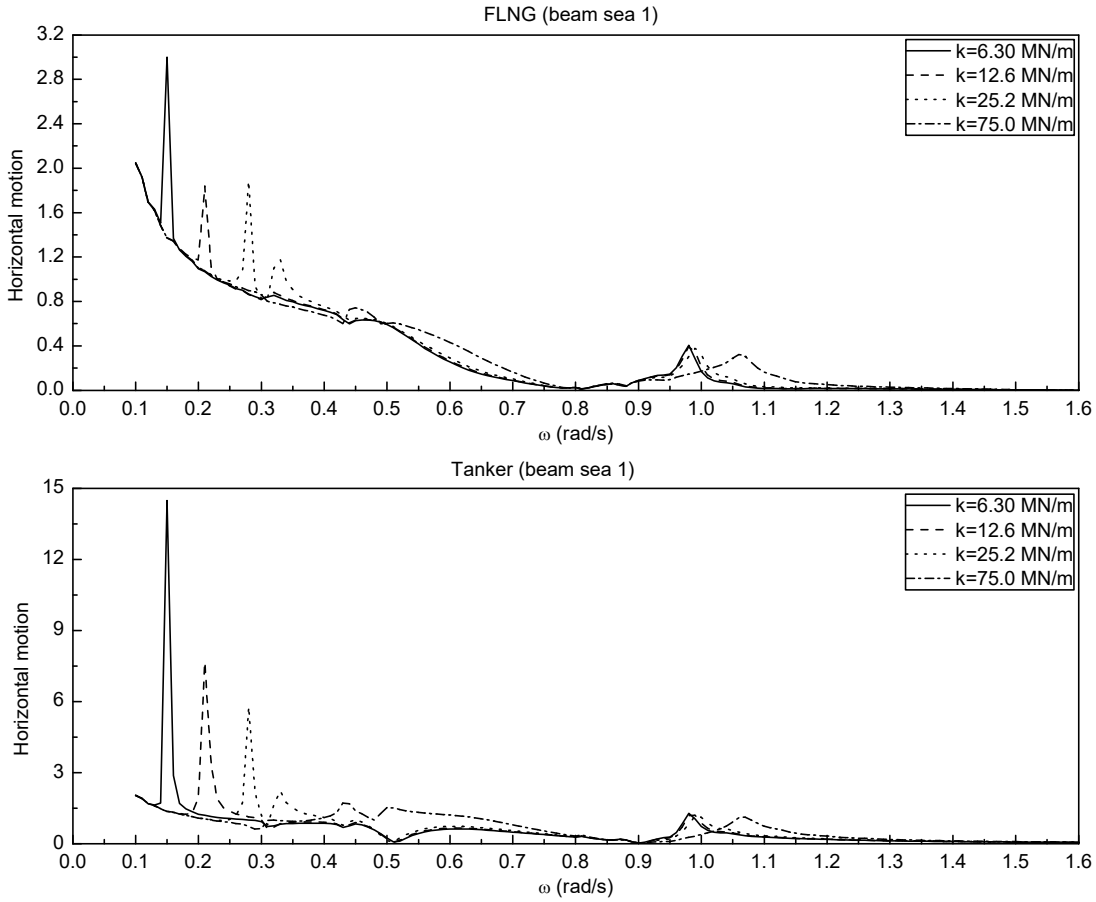

Figure 19. Horizontal responses in Beam Sea-1 for different spring stiffnesses

5. Conclusions

The Lagrange multiplier technique has been found to be very convenient for the analysis of multiple rigid bodies joined by rigid or flexible connections. In particular once the diffraction and radiation analyses have been performed, accounting for the

hydrodynamic interactions when the bodies are free to respond in their rigid body modes, the different responses under a variety of constraints may be very simply obtained. This also includes the possibility of the constraints being elastic. Results have been obtained using this approach for two geometries. One concerns two rectangular barges connected by either rigid or hinged bars, for which results have previously been given by Newman (1994). The comparisons are very satisfactory. This configuration also highlights the interesting result that because the problem is symmetric about a vertical plane through the centreline, there is no effect of the hinge on the vertical shear force in the connection.

The second geometry is that of a tanker alongside an FLNG barge, with a very small gap between the two vessels. This problem has previously been investigated by Sun et al. (2010b) for the case when the vessels are free to respond in all of their rigid body degrees of freedom, and the strong interactions associated with the small gap between them have been highlighted. Three further cases are considered here, involving different arrangements of constraints between the bodies. The influence of the interaction effects is again very considerable. Generally the behaviour of the vessels with rigid or hinged horizontal connections (cases 2 and 3) is fairly similar; and the freely floating and spring-connected configurations (cases 1 and 4) behave similarly. A very distinctive feature of the spring-connected arrangement is the large horizontal response of each vessel at low frequency (0.21 rad s^{-1} for the reference spring stiffness), which appears to be associated with a resonant mode in which the tanker oscillates horizontally relative to the large FLNG vessel. This is associated with a peak in the force in the spring; but this is much smaller than the peaks in the horizontal forces in the rigid and hinged connections just above 0.81 rad s^{-1}. It has been shown previously that this is the frequency of the largest peak in the frequency

response of the free surface elevation in the gap between the freely floating vessels. It is clear that the behaviour of the free surface in the gap is closely linked to the behaviour of the vessels and the forces in the connections.

Acknowledgements

The original hydrodynamic analysis for the unconstrained FLNG and LNG vessels was conducted under the auspices of the Safe Offload Project under EU Framework 6. Provision of facilities by the Oxford Supercomputing Centre is gratefully acknowledged.

We acknowledge the support of The Lloyd's Register Educational Trust towards the research and development programme in National University of Singapore.

References

Cheung, L. Y., 2010. Catamaran crane for EPCI contract. *IES Journal Part A: Civil & Structural Engineering*, in press.

Eatock Taylor, R., and Chau, F.P., 1992. Wave diffraction theory - some developments in linear and non-linear theory. *Transactions of ASME, Journal of Offshore Mechanics and Arctic Engineering*,114, 185-194.

Edelson, D., Luo, M., Halkyard, J. and Smiley, D., 2008. Kikeh development: spar floatover installation. In: *Proceedings of Offshore Technology Conference*, paper 19639, Houston, U. S. A.

Hong, S. Y., Kim, J. H., Cho, S. K., Choi, Y. R. and Kim, Y. S., 2005. Numerical and experimental study on hydrodynamic interaction of side-by-side moored multiple vessels. *Ocean Engineering*, 32, 783–801.

Koo, B. J., and Kim, M. H., 2005. Hydrodynamic interactions and relative motions of two floating platforms with mooring lines in side-by-side offloading operation. *Applied Ocean Research*, 27, 292–310.

Kashiwagi, M., 2007. 3-D calculation for multiple floating bodies in proximity using wave interaction theory. In: *Proceedings of the 17th International Conference on Offshore and Polar Engineering*, Lisbon, Portugal.

Kral, R. and Kreuzer, E., 1999. Multi-body systems and fluid-structure interactions with application to floating structures. *Multibody System Dynamics*, 3, 65–83.

Langley, R. S., 1984. Random dynamic analysis of multi-body offshore structures. *Ocean Engineering*, 11, 381–401.

Lee, C.-H. and Newman, J. N., 2000. An assessment of hydroelasticity for very large hinged vessels. *Journal of Fluids and Structures*, 14, 957-970.

Newman, J. N., (1994). Wave effects on deformable bodies. *Applied Ocean Research*, 16, 47-59.

Noble Denton Consultants Ltd., 2007. Design solution for LNG platforms. *NDC Report No: L22198/NDC/JK*, Safe Offload Document Identification Code 12-D-02-01.

Noble Denton Consultants Ltd., 2008. Design of mooring systems for vessel to vessel and vessel to GBS configurations (WP 5). *NDC Report No: L23202/NDC/XMC.*

O´'Catha´in, M., Leira, B. J., Ringwood, J. V. and Gilloteaux, J.-C., 2008. A modelling methodology for multi-body systems with application to wave-energy devices. *Ocean Engineering*, 35, 1381–1387.

Pauw, W. H., Huijsmans, R. H. M. and Voogt, A., 2007. Advances in the hydrodynamics of side-by-side moored vessels. In: *Proceedings of 26th International Conference on Offshore Mechanics and Arctic Engineering*, San Diego, USA.

Shabana, A. A., 2010. *Computational dynamics*. 3rd ed. Chichester: Wiley.

Sun, L., Taylor, P. H. and Eatock Taylor, R., 2010a. First- and second-order analysis of resonant waves between adjacent barges. *Journal of Fluids and Structures,* doi:10.1016/j.jfluidstructs.2010.06.001.

Sun, L., Taylor, P. H. and Eatock Taylor, R., 2010b. Free surface elevations in the gap between a tanker and a FLNG barge. Submitted for publication.

Sun, L., Teng, B., Liu, C. F., 2008. Removing irregular frequencies by a partial discontinuous higher order boundary element method. *Ocean Engineering*, 35, 920–930.

Tahar, A., Halkyard, J., Steen, A. and Finn, L., 2004. Float-over installation method – numerical and model test data. In: *Proceedings of 23rd International Conference on Offshore Mechanics and Arctic Engineering,* Vancouver, Canada.

Taghipour, R.and Moan, T., 2008. Efficient frequency-domain analysis of dynamic response for the multi-body wave energy converter in multi-directional waves. In: *Proceedings of 18th Offshore and Polar Engineering Conference*, Vancouver, Canada.

Zang, J., Gibson, R., Taylor, P. H., Eatock Taylor, R. and Swan, C., 2006. Second order wave diffraction around a fixed ship-shaped body in unidirectional steep waves. *Transactions of ASME, Journal of Offshore Mechanics and Arctic Engineering*, 128, 89-99.